IEEE Photonics Journal
An IEEE Photonics Society Publication

Open Access

Transmission Enhancement in Coaxial Hole Array Based Plasmonic Color Filter for Image Sensor Applications

Volume 10, Number 4, August 2018

Xin He
Nicholas O'Keefe
Yajing Liu
Dechuan Sun
Hemayet Uddin
Ampalavanapillai Nirmalathas
Ranjith Rajasekharan Unnithan

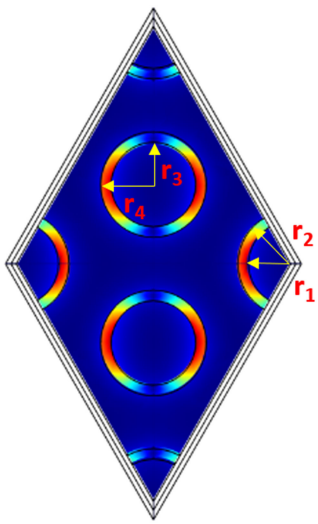

Dual Coaxial Hole Array (DCHA)

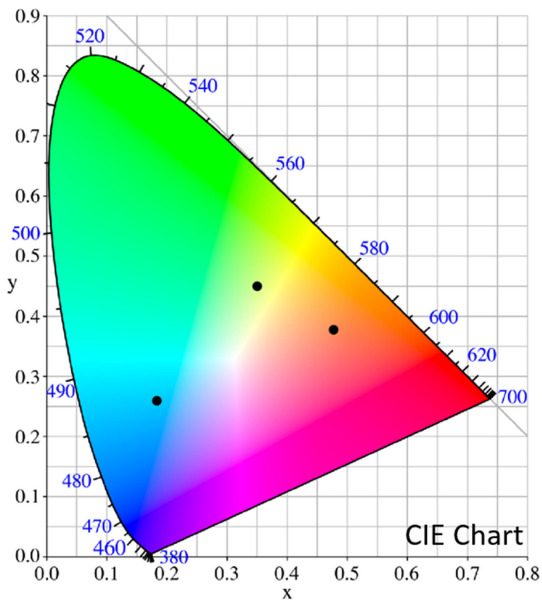

DOI: 10.1109/JPHOT.2018.2855684
1943-0655 © 2018 IEEE

Transmission Enhancement in Coaxial Hole Array Based Plasmonic Color Filter for Image Sensor Applications

Xin He,[1] Nicholas O'Keefe,[1] Yajing Liu,[1] Dechuan Sun,[1] Hemayet Uddin,[2] Ampalavanapillai Nirmalathas,[1] and Ranjith Rajasekharan Unnithan [1]

[1]Department of Electrical and Electronic Engineering, The University of Melbourne, Melbourne, VIC 3010, Australia
[2]Melbourne Centre for Nanofabrication, Australian National Fabrication Facility, Clayton, VIC 3168, Australia

DOI:10.1109/JPHOT.2018.2855684

Manuscript received May 9, 2018; revised July 3, 2018; accepted July 9, 2018. Date of publication July 26, 2018; date of current version August 6, 2018. The work of R. R. Unnithan was supported by ARC Project LP160101475. Corresponding author: Ranjith Rajasekharan Unnithan (e-mail: r.ranjith@unimelb.edu.au).

Abstract: Plasmonic color filters based on the hexagonal arrangement of coaxial hole array in aluminum have been demonstrated as a promising candidate for color filter development due to polarization and incident angle insensitivity. They also comprise a single nanometer thick metal film, demonstrate good line width, CMOS compatibility, and fine color tunability. However, the low transmittance of the coaxial hole array based filters limits their use in potential applications such as image sensors and displays. This paper introduces a new method to increase transmittance in coaxial hole array based filters by tuning localized surface plasmons and surface plasmon polaritons. In this method, coaxial holes of small diameters are filled along with a large size coaxial hole array to form a combined filter geometry with optimized parameters in aluminum film using computational techniques. The simulation results will have potential applications in CMOS image sensors, submicron pixel development, microdisplays, and liquid crystal over silicon devices.

Index Terms: Plasmonic colour filter, coaxial hole array, localized surface plasmon.

1. Introduction

As demand for high-resolution imagery continues to expand in consumer, scientific and industrial applications there is a need for smaller, highly tunable and robust colour filters [1]–[4]. Precise control of wavelength provides vivid colour response and improved selectivity. CMOS image sensor technologies have undergone enormous advances in recent years to increase performance and reduce pixel size. Along with reducing the transistor size to nanoscale for image sensors, submicron scale filters are also required to perform filtering for image acquisition sensors, next generation spatial light modulators [5]–[7] and high-resolution microdisplays.

Conventional colour filters are made from pigments and dyes. The filter colour response is directly related to the absorption coefficient, which in turn is related to the area/volume of the filters. Therefore, it is difficult to make nanometer-sized colour filters using pigments and dyes [1]–[4], [8], [9]. Recently, colour filters based on the titanium oxide nanodisk operating in reflection mode were reported as having good optical performance because of its low loss and high refractive

index in the visible range [10]. However, this design is not suitable for image sensor applications due to their operation in reflection mode. Moreover, the titanium oxide nanodisk is not CMOS compatible. Plasmonic colour filters based on aluminium are better candidates to most of the all-dielectric colour filters due to their CMOS compatibility, ability to operate in transmission mode, use of single namometer thick film and excellent colour tunability (from UV to NIR range) [1], [8], [11]. Furthermore, the filter spectral response can be carefully controlled by parameterising structure geometry, producing artificial material properties engineered to specific design and application requirements. There have been many demonstrations of colour filters employing plasmonic effects in the literature, especially using nanostructures in thin metal film [1]–[4], [8], [9], [11]–[30]. Such colour filters can be fabricated using a single perforated metal film with the thickness of 50 to 200 nm. Despite these promising attributes, plasmonic filters still suffer from the poor transmission and incident angle sensitivity which have limited the scope of target applications and increased deployment requirements in CMOS and display applications. For example, the peak transmittance wavelength for a simple hole array based plasmonic colour filters depends on the angle of the incident light because the surface plasmons based effect in the hole array is angle sensitive [8], [24]. If such a hole array filter were used in an image sensor, the filter will transmit only the desired colour at normal incidence while different colors would be filtered at oblique incidences.

Plasmonic colour filters based on the coaxial holes were reported using gold (Au) [12]. However, the coaxial hole array in Au film is limited to produce the resonance peak at wavelengths less than 480 nm [12] due to the material limitation [13]. It has been demonstrated that transmittance of a square aperture array in the silver film can be enhanced using suitably placed small squares [27], however, the square aperture is polarization sensitive. Other designs were reported by creating symmetric patterns inserted into the metal film to increase the transmittance, such as the nano trench or cavity [28], [29]. Extra coating on the Ag-Si film was also demonstrated to enhance the transmittance [30] based on the Fabry–Pérot resonances. However, these demonstrated structures are not covering full colours in the visible range, and Ag oxidizes in air. Au and Ag based filters are not CMOS compatible and also require a seed layer for better adhesion to substrates which increases the fabrication complexity.

Recently, it has been reported that vivid red, green and blue colours could be produced by plasmonic colour filters based on the hexagonal arrangement of coaxial holes in aluminium [11] and it is a promising candidate for image sensor applications, due to its angle insensitive and polarization independent characteristics. However, the transmittance of colour filters based on coaxial hole arrays is too low to be used in an image sensor or display as the transmittance reported in the literature varies from 5% (red) to more than 20% (blue) [11]. This is because, for the localized surface plasmon, peak wavelength depends on gap size, thus as the gap decreases a shift towards the red region is introduced. Therefore, it is important to develop techniques to increase the transmittance of plasmonic colour filters without compromising important characteristics such as polarization and incident angle insensitivity, good line width, fine tuning capability and CMOS compatibility.

In this paper, we present a technique to enhance transmittance of plasmonic colour filters based on the coaxial hole array in aluminium. We demonstrate a new scheme to overcome the limitation of low transmittance in the coaxial hole array filter using two different coaxial holes geometry that is independently tuned to the same colour (wavelength), followed by merging both the coaxial geometries to make a combined geometry.

2. Simulation Model and Optimization Method

The plasmonic resonance peaks responsible for obtaining different colours in a coaxial geometry are predominantly due to localized surface plasmons (Fabry–Pérot resonances) supported in a cylindrical resonance cavity. The cavity is excited by cylindrical surface plasmons formed by a metal film with finite thickness and two end faces. Tuning of colours was obtained by varying inner (r_1) and outer (r_2) radii of the coaxial hole using localized surface plasmons. The resonance peak (peak transmittance wavelength) can be obtained using different combinations of the inner (r_1)

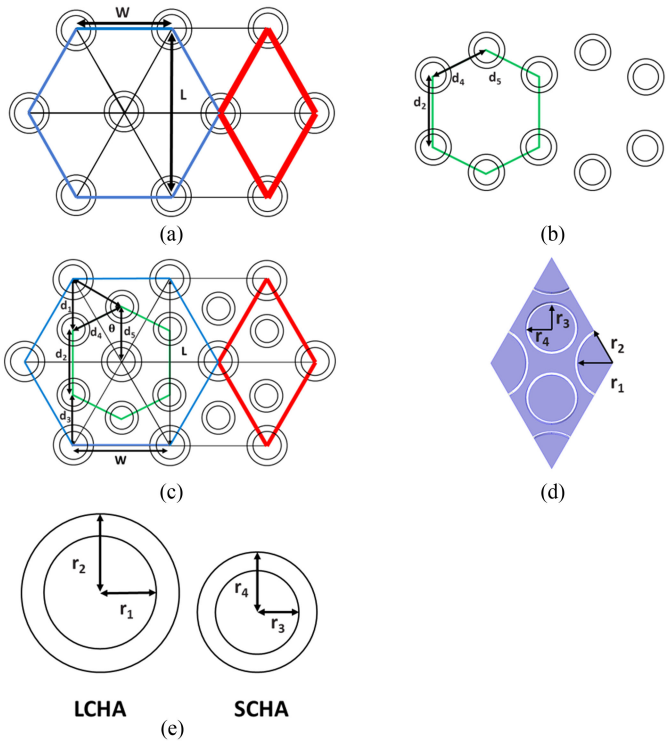

Fig. 1. Schematic of (a) Large coaxial hole array (LCHA): Coaxial hole array showing a unit cell (red) used for simulation. Periodic boundary condition was used on four sides to simulate an array (b) Small coaxial hole array (SCHA) (c) Dual coaxial hole array (DCHA) made of a combination of large coaxial hole array (LCHA) and small coaxial hole array (SCHA) (d) Top view of DCHA unit cell (e) The radius of LCHA and SCHA.

and outer radii (r_2) as shown in Fig. 1. The desired colour (transmittance peak) can be calculated using the equation $l = (n\pi - \Omega)/\beta$ [8], [9], [14], where l, n, Ω and β are the thickness of the metal film, the order of the Fabry-Pérot resonance, the phase of reflection constant and the propagation constant respectively. There is also a minor contribution to resonance peaks in the coaxial hole array geometry due to the pitch between coaxial holes caused by surface plasmons polaritons [11], [12]. Here, we have exploited both the tuning of localized surface plasmons and surface plasmons for obtaining RGB colours.

The coaxial hole array in the hexagonal arrangement was simulated using a unit cell of a regular hexagon as shown in Fig. 1(a) where W and L are defined as the separation between large coaxial holes in x and y directions respectively. The relationship between W and L are chosen such as $L = 2 \times W \times \frac{\sqrt{3}}{2} = \sqrt{3}W$ for producing hexagonal geometry. To increase the transmittance, hexagonal geometry of large coaxial holes array (LCHA in blue regular hexagon block in Fig. 1(a)) is combined with an additional coaxial hole array with a smaller radius (SCHA in Fig. 1(b)) to create a dual coaxial hole array (DCHA) in such a way that the combined geometry is polarization insensitive. In DCHA, the distance between two adjacent small coaxial holes is the same as the length d_1, the distance between the adjacent large coaxial hole and small coaxial hole. With the angle $\theta = 60^\circ$, as a result, $d_1 = d_2 = d_3 = d_4 = d_5 = \frac{1}{3}L = \frac{\sqrt{3}}{3}W$ as shown in Fig. 1(c). The 3D geometries are computationally investigated using the finite element method (FEM) implemented in COMSOL MULTIPHYSICS. The simulation unit is highlighted by the red diamond block in Fig. 1(c) and its top view is shown in Fig. 1(d). The simulation model consists of a 150 nm thick layer of aluminium on a semi-infinite glass substrate ($n = 1.5$) with 200 nm thickness to find the wavelength at which maximum transmittance occurs for the filters. The top layer is air with a thickness of 200 nm. Light is

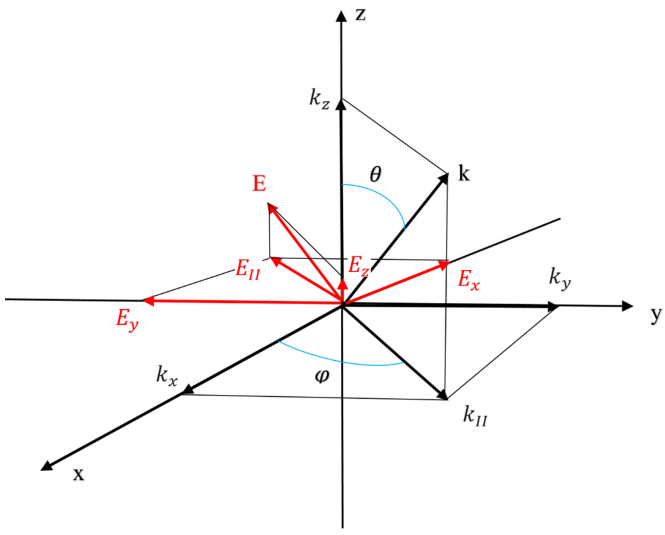

Fig. 2. Schematic of incident plane wave: k is the propagation constant, θ is the angle of incidence and φ is the polarization angle.

excited from the aluminium side (top side) using port boundary conditions. S-parameters are used to find the transmittance ($|S21|^2$) of the filters. Perfectly matched layer (PML) is used on the top and at the bottom of the model to avoid effects of reflected light in the transmittance spectrum.

Details of the incident wave are shown in Fig. 2, and formula for electric field to study polarization and angle sensitivity is given below [31].

$$\mathrm{E}_x = \mathrm{A}\sin\left(\frac{\pi}{2}-\theta\right)\cos(\pi+\varphi)\,\mathrm{e}^{-\mathrm{j}(\mathrm{k}_x\cdot\mathrm{x}+\mathrm{k}_y\cdot\mathrm{y}+\mathrm{k}_z\cdot\mathrm{z})},$$

$$\mathrm{E}_y = \mathrm{A}\sin\left(\frac{\pi}{2}-\theta\right)\sin(\pi+\varphi)\,\mathrm{e}^{-\mathrm{j}(\mathrm{k}_x\cdot\mathrm{x}+\mathrm{k}_y\cdot\mathrm{y}+\mathrm{k}_z\cdot\mathrm{z})},$$

$$\mathrm{E}_z = \mathrm{A}\cos\left(\frac{\pi}{2}-\theta\right)\mathrm{e}^{-\mathrm{j}(\mathrm{k}_x\cdot\mathrm{x}+\mathrm{k}_y\cdot\mathrm{y}+\mathrm{k}_z\cdot\mathrm{z})},$$

$$|\mathrm{E}| = \sqrt{\mathrm{E}_x^2+\mathrm{E}_y^2+\mathrm{E}_z^2} = \mathrm{A},\ \mathrm{k}_x = \mathrm{k}\sin\theta\cos\varphi,\ \mathrm{k}_y = \mathrm{k}\sin\theta\sin\varphi,\ \mathrm{k}_z = \mathrm{k}\cos\theta.$$

The θ is the incident angle, φ is the polarization angle which is in the direction of $\mathrm{E}_{//}$. Propagation constant k is defined as $(2\pi \times n)/\lambda$ where n is the refractive index of the simulation domain (air) where the port is set for illumination. The refractive indices of aluminium at different wavelengths are taken from Palik's experiment [32]. The incident angle θ was varied to study the effect of transmittance with respect to the angle of incidence. Similarly, polarization angle φ was varied to study polarization sensitivity.

3. Results

Based on the simulation models discussed above, in the first step, a large coaxial hole array is designed to produce the peak wavelength of 650 nm (red colour filter) by tuning inner (r_1) and outer (r_2) radii to 120 nm and 130 nm, respectively by tuning the localized surface plasmons. This is followed by tuning the pitch to 420 nm for $\mathrm{LCHA_R}$ by tuning LSP. $\mathrm{LCHA_R}$ gives a transmittance of 6.2% and a line width of 180 nm (FWHM). In the second step, another small coaxial hole array is designed to the same peak wavelength of 650 nm by tuning inner and outer radii to 83 nm and 90 nm, respectively ($\mathrm{SCHA_R}$). $\mathrm{SCHA_R}$ gives a 5.6% transmittance with FWHM of 150 nm. In the final step, both $\mathrm{LCHA_R}$ and $\mathrm{SCHA_R}$ are combined to create the dual coaxial hole array ($\mathrm{DCHA_R}$) with the

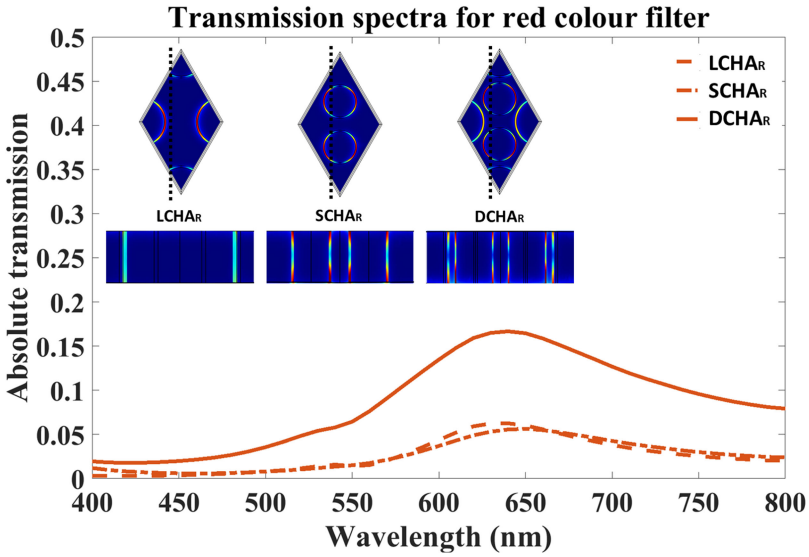

Fig. 3. Red colour filter: Transmission spectra of large coaxial hole array ($LCHA_R$), small coaxial hole array ($SCHA_R$) and dual coaxial hole array ($DCHA_R$). Subset images show normalized electric field from top view and lateral cross section along the dotted black line for $LCHA_R$, $SCHA_R$ and $DCHA_R$.

enhanced transmittance of 15.5% with FWHM of 215 nm. These results are presented in Fig. 3. The insets of the Fig. 3 show normalized electric field on $LCHA_R$, $SCHA_R$ and $DCHA_R$ which shows that both large and small coaxial hole arrays are excited by the incident light, and both are contributing to transmission. The increased transmittance is due to the coupling of plasmon resonances in both large and small coaxial holes constructively by geometrical tuning.

RGB colours are required for making the bayer pattern in CMOS image sensors. Hence the same scheme used for the red colour is applied for both green and blue colour filters. The blue colour ($LCHA_B$) is obtained by tuning the pitch size to 260 nm, and radii to $r_1 = 40$ nm and $r_2 = 50$ nm. $LCHA_B$ is then combined with a small coaxial hole array tuned to the same wavelength ($SCHA_B$) with $r_3 = 40$ nm, $r_4 = 50$ nm to obtain $DCHA_B$. For the green colour ($LCHA_G$), pitch size is 430 nm, r_1 and r_2 are 106 nm and 130 nm respectively. Then combining another smaller coaxial hole array ($SCHA_G$) with $r_3 = 70$ nm, $r_4 = 80$ nm for the green colour ($DCHA_G$).

The transmission spectra of blue and green colour filter for LCHA, SCHA and DCHA are shown in Fig. 4 and Fig. 5 respectively, and their line widths (FWHM) are tabulated in Table 1. CIE 1931 chromaticity diagram was plotted for red, green and blue colour filters using chromaticity coordinates obtained from simulation results for LCHA and DCHA (Fig. 6). The CIE chromaticity chart shows that the pure colour perceived by human vision is obtained from the spectrum of different colour filters. From the CIE chromaticity charts of LCHA and DCHA, it is shown that the measured chromaticity coordinates of the RGB filters falls around the achromatic point. For the green and red DCHA colour filters, their positions are slightly shifted on the CIE chart towards the center (white light) compared to LCHA. But the shift is still falling around the achromatic point and is within the acceptable limit. This effect is due to a slight increase in FWHM after combining LCHA and SCHA. This demonstrates the capability of DCHA based colour filters with increased transmittance for a large degree of colour range tuning applications such as CMOS image sensors.

There are two important requirements for a colour filter to be used in CMOS image sensors, viz polarization insensitivity and angle independence. The polarization insensitivity ensures capturing the exact colour and intensity of objects irrespective of the rotation of camera/sensor. Angle independence is essential to obtain the same colour of objects irrespective of the angle of recording. For example, if the filters are angle sensitive, the same object will be recorded with different colours at different angles of the image capture. The transmittance of DCHA is studied for three different

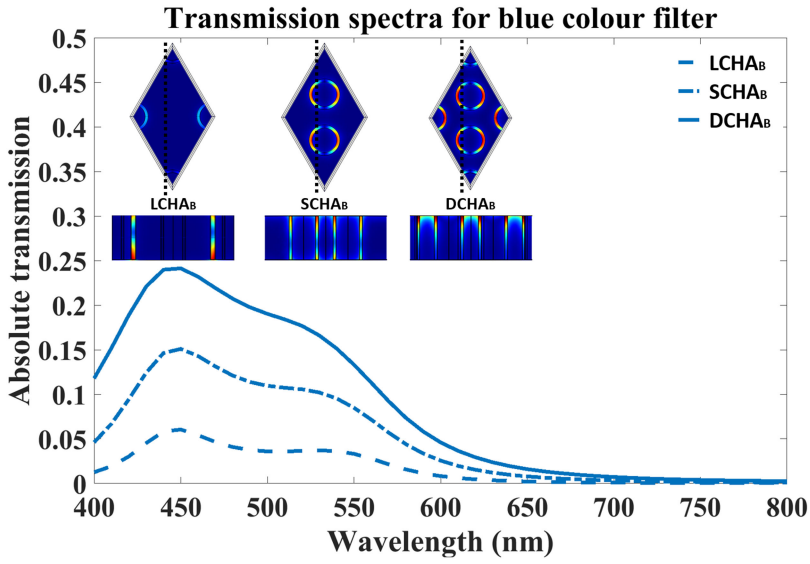

Fig. 4. Blue colour filter: Transmission spectra of large coaxial hole array ($LCHA_B$), small coaxial hole array ($SCHA_B$) and dual coaxial hole array ($DCHA_B$). Subset images show normalized electric field from top view and lateral cross section along the dotted black line for $LCHA_B$, $SCHA_B$ and $DCHA_B$.

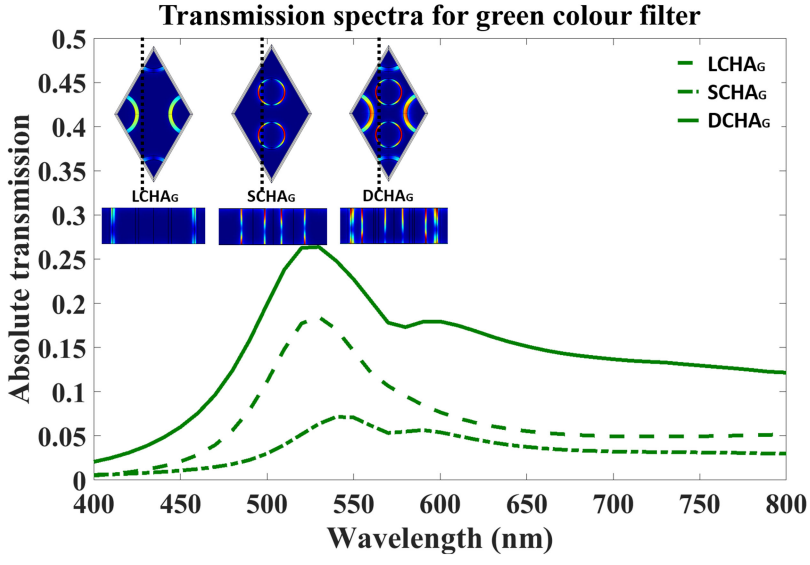

Fig. 5. Green colour filter: Transmission spectra of large coaxial hole array ($LCHA_G$), small coaxial hole array ($SCHA_G$) and dual coaxial hole array ($DCHA_G$). Subset images show normalized electric field from top view and lateral cross section along the dotted black line for $LCHA_G$, $SCHA_G$ and $DCHA_G$.

polarization angles, 0°, 45° and 90°. A red DCHA colour filter ($DCHA_R$) is taken as an example as shown in Fig. 7(a). The results show the DCHA is almost polarization insensitive. Furthermore, transmission characteristics of the red colour DCHA are studied for different incident angles (full field angle: FFOV), 0°, 30° and 60°, as shown in Fig. 7(b). There is no shift in the peak wavelength with respect to angle, and hence the transmitted colour will be the same from different angles of illumination with a small reduction in the intensity (∼3.5%). These results show that DCHA design is very promising for colour filter development due to angle insensitivity, polarization insensitivity, good line width (FWHM), fine tuning ability and CMOS compatibility.

TABLE 1
Maximum Transmittance, Peak Wavelength and FWHM for LCHA, SCHA and DCHA of Blue, Green and Red Colour Filter

Colour	Model	Maximum transmittance	Peak wavelength	FWHM
Blue	$LCHA_B$	6.0%	450nm	140nm
	$SCHA_B$	15.0%	450nm	150nm
	$DCHA_B$	24%	450nm	150nm
Green	$LCHA_G$	18.4%	530nm	120nm
	$SCHA_G$	7.1%	530nm	180nm
	$DCHA_G$	26.4%	530nm	200nm
Red	$LCHA_R$	6.2%	650nm	180nm
	$SCHA_R$	5.6%	650nm	150nm
	$DCHA_R$	15.5%	650nm	215nm

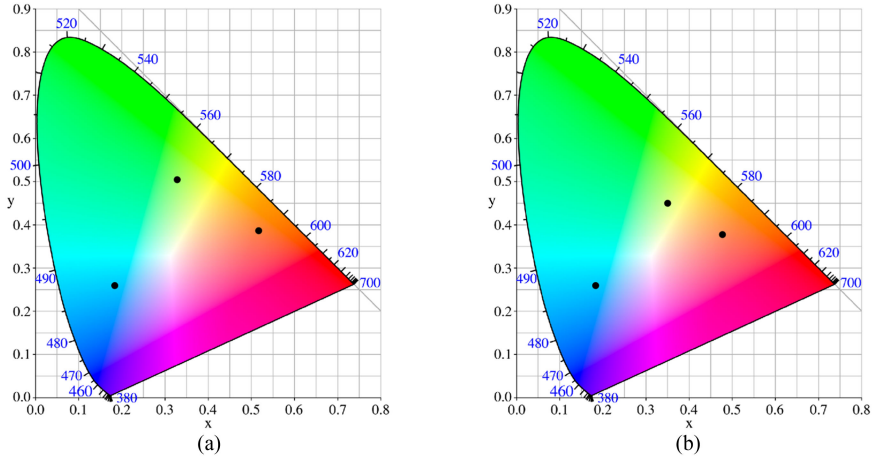

Fig. 6. CIE chromaticity chart of blue, green and red colour filter for (a) LCHA, and (b) DCHA.

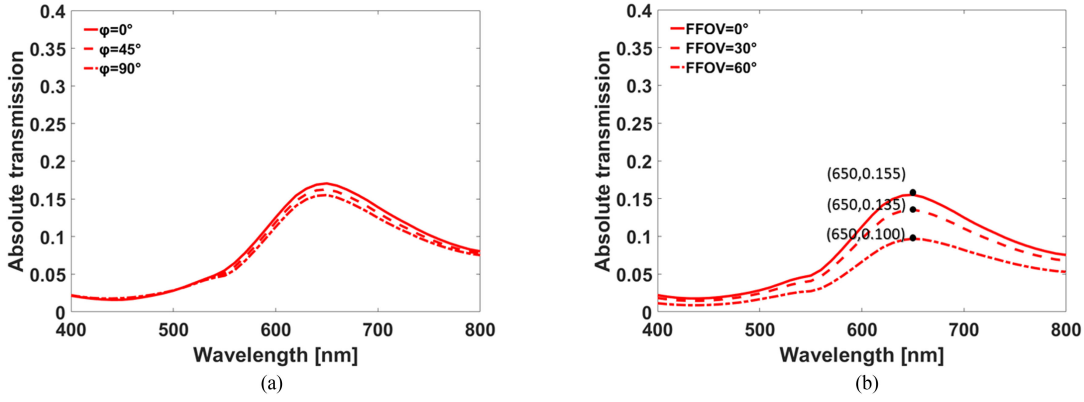

Fig. 7. Transmission spectrum of DCHA for different polarizations and angle of excitations (a) the polarization angles $\varphi = 0^\circ$, $\varphi = 45^\circ$, $\varphi = 90^\circ$ and corresponding transmission spectra showing DCHA is polarization insensitive (b) angle dependence of DCHA shows no shift in peak wavelength with respect to angle and variation in transmittance is negligible. Here, the angle of incidence (excitation) represented as full field of view (full angle), FFOV $= 0^\circ, 30^\circ, 60^\circ$.

4. Conclusion

The paper presents a technique to increase peak transmittance of the hexagonal arrangement of coaxial hole array in aluminium without compromising its polarization insensitivity, line width and angle insensitivity. In the proposed technique, one large coaxial hole array is designed for a peak wavelength of interest after optimization, followed by designing a small coaxial hole array to the same peak wavelength. These two coaxial hole arrays are then combined in a suitable fashion to enhance the transmittance. The transmittance is increased more than 2x for red colour filter, 1.4x for green colour and 4x for blue colour. These results will have potential applications in developing micron and submicron colour filter development for CMOS sensors, micro-displays and spatial light modulators.

Acknowledgment

This research/project was undertaken with the assistance of resources and services from the National Computational Infrastructure (NCI), which is supported by the Australian Government.

References

[1] S. Yokogawa, S. P. Burgos, and H. A. Atwater, "Plasmonic color filters for CMOS image sensor applications," *Nano Lett.*, vol. 12, no. 8, pp. 4349–4354, 2012.
[2] Q. Chen, D. Chitnis, K. Walls, T. D. Drysdale, S. Collins, and D. R. S. Cumming, "CMOS photodetectors integrated with plasmonic color filters," *IEEE Photon. Technol. Lett.*, vol. 24, no. 3, pp. 197–199, Feb. 2012.
[3] S. P. Burgos, S. Yokogawa, and H. A. Atwater, "Color imaging via nearest neighbor hole coupling in plasmonic color filters integrated onto a complementary metal-oxide semiconductor image sensor," *ACS Nano*, vol. 7, no. 11, pp. 10038–10047, 2013.
[4] Y. Yu, Q. Chen, L. Wen, X. Hu, and H. F. Zhang, "Spatial optical crosstalk in CMOS image sensors integrated with plasmonic color filters," *Opt. Exp.*, vol. 23, no. 17, pp. 21994–22003, 2015.
[5] Q. Dai, R. Rajasekharan, H. Butt, K. Won, and X. Z. Wang, "Transparent liquid-crystal-based microlens array using vertically aligned carbon nanofiber electrodes on quartz substrates," *Nanotechnology*, vol. 22, no. 11, 2011, Art. no. 115201.
[6] R. Rajasekharan, T. D. Wilkinson, P. J. W. Hands, and Q. Dai, "Nanophotonic three-dimensional microscope," *Nano Lett.*, vol. 11, no. 7, pp. 2770–2773, 2011.
[7] R. Rajasekharan, C. Bay, Q. Dai, J. Freeman, and T. D. Wilkinson, "Electrically reconfigurable nanophotonic hybrid grating lens array," *Appl. Phys. Lett.*, vol. 96, 2010, Art. no. 233108.
[8] R. R. Unnithan *et al.*, "Filling schemes at submicron scale: Development of submicron sized plasmonic colour filters," *Sci. Rep.*, vol. 4, 2014, Art. no. 6435.
[9] T. H. Hsu *et al.*, "Light guide for pixel crosstalk improvement in deep submicron CMOS image sensor," *IEEE Electron Device. Lett.*, vol. 25, no. 1, pp. 22–24, Jan. 2004.
[10] B. Yang, W. W. Liu, Z. C. Li, H Cheng, S. Q. Chen, and J. G. Tian, "Polarization-sensitive structural colors with hue-and-saturation tuning based on all-dielectric nanopixels," *Adv. Opt. Mater.*, vol. 6, 2018, Art. no. 1701009.
[11] R. R. Unnithan *et al.*, "Plasmonic colour filters based on coaxial holes in aluminium," *Materials*, vol. 10, no. 4, 2017, Art. no. E383.
[12] G. Y. Si *et al.*, "Annular aperture array based color filter," *Appl. Phys. Lett.*, vol. 99, 2011, Art. no. 033105.
[13] W. K. Mark, S. K. Nicholas, L. F. Liu, O. E. Henry, N. Peter, and J. H. Naomi, "Aluminum for plasmonics," *ACS Nano*, vol. 8, no. 1, pp. 834–840, 2014.
[14] L. B. Sun *et al.*, "Effect of relative nanohole position on colour purity of ultrathin plasmonic substractive colour filters," *Nanotechnology*, vol. 26, no. 30, 2015, Art. no. 305204.
[15] C. Genet and T. W. Ebbesen, "Light in tiny holes," *Nature*, vol. 445, pp. 39–46, 2007.
[16] D. Inoue *et al.*, "Polarization independent visible color filter comprising an aluminum film with surface-plasmon enhanced transmission through a subwavelength array of holes," *Appl. Phys. Lett.*, vol. 98, 2011, Art. no. 093113.
[17] B. Heshmat, D. Li, T. E. Darcie, and R. Gordon, "Tuning plasmonic resonances of an annular aperture in metal plate," *Opt. Exp.*, vol. 19, pp. 5912–5923, 2011.
[18] W. Liu *et al.*, "Complete spectral gap in coupled dielectric waveguides embedded into metal," *Appl. Phys. Lett.*, vol. 97, 2010, Art. no. 021106.
[19] Q. Chen and D. R. S. Cumming, "High transmission and low color cross-talk plasmonic color filters using hexagonal-lattice hole arrays in aluminum films," *Opt. Exp.*, vol. 18, no. 13, pp. 14056–14062, 2010.
[20] M. Najiminaini, F. Vasefi, B. Kaminska, and J. J. L. Carson, "Nanohole-array-based device for 2D snapshot multispectral imaging," *Sci. Rep.*, vol. 3, 2013, Art. no. 2589.
[21] H. S. Lee, Y. T. Yoon, S. S. Lee, S. H. Kim, and K. D. Lee, "Color filter based on a subwavelength patterned metal grating," *Opt. Exp.*, vol. 15, no. 23, pp. 15457–15463, 2007.
[22] H. J. Lezec and T. Thio, "Diffracted evanescent wave model for enhanced and suppressed optical transmission through subwavelength hole arrays," *Opt. Exp.*, vol. 12, no. 16, pp. 3629–3651, 2004.

[23] Q. Chen, D. Chitnis, K. Walls, T. D. Drysdale, S. Collins, and D. R. S. Cumming, "CMOS photodetectors integrated with plasmonic color filters," *IEEE Photon. Technol. Lett.*, vol. 24, no. 3, pp. 197–199, Feb. 2012.
[24] S. Balakrishnan, M. Najiminaini, M. R. Singh, and J. J. L. Carson, "A study of angle dependent surface plasmon polaritons in nano-hole array structures," *J. Appl. Phys.*, vol. 120, 2016, Art. no. 034302.
[25] B. B. Zeng, Y. K. Gao, and F. J. Bartoli, "Ultrathin nanostructured metals for highly transmissive plasmonic subtractive color filters," *Sci. Rep.*, vol. 3, 2013, Art. no. 2840.
[26] B. Y. Zheng, Y. M. Wang, P. Nordlander, and N. J. Halas, "Color-selective and CMOS-compatible photodetection based on aluminum plasmonics," *Adv. Mater.*, vol. 26, no. 36, pp. 6318–6323, 2014.
[27] X. N. Zhang *et al.*, "Effects of compound rectangular subwavelength hole arrays on enhancing optical transmission," *IEEE Photon. J.*, vol. 7, no. 1, Feb. 2015, Art. no. 4500408.
[28] C. M. Wang, H. I. Huang, C. C. Chao, J. Y. Chang, and Y. Sheng, "Transmission enhancement through a trench-surrounded nano metallic slit by bump reflectors," *Opt. Exp.*, vol. 15, no. 6, pp. 3496–3501, 2007.
[29] H. Lu, X. M Liu, Y. K Gong, D. Mao, and L. R Wang, "Enhancement of transmission efficiency of nanoplasmonic wavelength demultiplexer based on channel drop filters and reflection nanocavities," *Opt. Exp.*, vol. 19, no. 14, pp. 12885–12890, 2011.
[30] Q. Li *et al.*, "Transmission enhancement based on strong interference in metal-semiconductor layered film for energy harvesting," *Sci. Rep.*, vol. 6, 2016, Art. no. 29195.
[31] "Setting excitation in 3D," [Online]. Available: http://srdjancomsol.weebly.com/setting-excitation-in-3d.html
[32] E. D. Palik, *Handbook of Optical Constants*. San Diego, CA, USA: Academic, 1998.